Cement and Concrete Research 40 (2010) 1320–1326

Contents lists available at ScienceDirect

Cement and Concrete Research

journal homepage: http://ees.elsevier.com/CEMCON/default.asp

# Appraisal of a cementitious material for waste disposal: Neutron imaging studies of pore structure and sorptivity

Peter J. McGlinn [a,*], Frikkie C. de Beer [b], Laurence P. Aldridge [a], Mabuti J. Radebe [b], Robert Nshimirimana [b], Daniel R.M. Brew [a], Timothy E. Payne [a], Kylie P. Olufson [a]

[a] Australian Nuclear Science and Technology Organisation, New Illawarra Road, Lucas Heights, NSW 2234, Australia
[b] South African Nuclear Energy Corporation (Necsa), Church Street West Extension, Pelindaba, Brits District, Pretoria 0001, South Africa

ARTICLE INFO

*Article history:*
Received 27 May 2009
Accepted 15 March 2010

*Keywords:*
B Characterization
B Pore size distribution
B Tomography
C Transport properties
E Radioactive waste

ABSTRACT

Cementitious materials are conventionally used in conditioning intermediate and low level radioactive waste. In this study a candidate cement-based wasteform has been investigated using neutron imaging to characterise the wasteform for disposal in a repository for radioactive materials. Imaging showed both the pore size distribution and the extent of the cracking that had occurred in the samples. The rate of the water penetration measured both by conventional sorptivity measurements and neutron imaging was greater than in pastes made from Ordinary Portland Cement. The ability of the cracks to distribute the water through the sample in a very short time was also evident.

The study highlights the significant potential of neutron imaging in the investigation of cementitious materials. The technique has the advantage of visualising and measuring, non-destructively, material distribution within macroscopic samples and is particularly useful in defining movement of water through the cementitious materials.



## 1. Introduction

Cementitious material is the most commonly used medium in the safe disposal of low and intermediate level radioactive waste. It may be used both as a barrier to prevent water from contacting the radioactive nuclides, and as an encapsulant against the migration of radionuclides. In practice both depend on limiting water transport and therefore the movement of water through the cementitious barrier is of fundamental importance to predicting the performance of cementitious wasteform.

This paper focuses on water transmission of a well-characterised candidate wasteform, one un-leached and the other leached for almost 8 years. In work already reported [1] a series of short to long term (up to 8 years) durability tests were conducted on this waste-form and the leaching tests were complemented by surface characterisation (using Scanning Electron Microscopy and Secondary Ion Mass Spectrometry) and bulk mineralogical analysis (X-ray Diffraction).

Understanding water transportation through the cementitious material is important to predict and control its service lifetime. Water transportation is controlled largely by porosity, cracking (pore connectivity) and initial water content. In the work reported here, water transport through a wasteform cement was monitored using the techniques of sorptivity [2,3] and neutron radiography (NR) [4–6]. Neutron radiography (NR) permits non-destructive, quantitative analysis of hydrogenous material due to the contrasting neutron attenuation within the material under investigation. NR was used to determine the overall rate of water transport in 2-D and neutron tomography (NCT) allowed an insight into paths of water transport in 3-D. Sorptivity measures the rate of water ingress into the wasteform and this rate is related to the size of the paths that water can travel in the sample, thereby giving the bulk or average path. Neutron radiographs of the wasteforms also visualise the extent of the water front within the sample. Provided the cracks or pores are larger than the effective resolution limit used in the neutron imaging then the rate of the water transmission *in situ* as the pores and cracks are filling can be followed.

The aim of this work was to investigate water transport in a candidate cementitious wasteform. Further work was undertaken so that the results of this study could be directly related to the performance of pure cement pastes.

## 2. Experimental

### 2.1. Wasteform material and sample conditioning

The samples tested simulated the Materials Testing Reactor (MTR) wasteform (produced at the Dounreay Cementation Plant in Scotland),

* Corresponding author.
*E-mail address:* pjm@ansto.gov.au (P.J. McGlinn).

0008-8846/$ – see front matter. 
doi:10.1016/j.cemconres.2010.03.011

a candidate cementitious material resulting from conditioning of intermediate level waste. The wasteform has a formulation of 9:1 ground granulated blast furnace slag to Ordinary Portland Cement (OPC) and has a white surface layer different in appearance to the underlying matrix. Whilst the real waste contains a number of fission products [7] the wasteform studied in this work was made from simulated waste liquor. The waste liquor contained salts dissolved in $H_2SO_4$ and neutralised in caustic solution [8].

The samples were supplied in the form of cylinders about 8 cm high and 4 cm in diameter. One sample was un-leached and the other had been leached for almost 8 years, at 40 °C for the first 12 months and thereafter at room temperature. This comparison was made to determine the effect of long term contact of the MTR wasteform with water on subsequent water transmissivity properties.

Previous studies [1] showed the MTR samples to be characteristically white on the outside (to a depth of 800 μm) and mottled grey beneath the surface layer. XRF analysis showed the surface layer was richer in Na and K, and poorer in S and Ca than the bulk interior samples. The other elements appeared to be in equal concentrations in all samples. X-ray Diffraction showed the presence of calcite, hydrotalcite and a calcium silicate hydrate, with the white exterior layer significantly richer in calcite than the interior. SEM/EDS (Energy Dispersive X-ray Spectrometry) showed a high degree of inhomogeneity in the wasteform with observations of the leached samples reflecting a dissolution front that left a zone of decalcified CSH surrounding an uncorroded core [9].

The cement specimens were dried at 50 °C to constant weight to remove excess free water whilst retaining pore structure, prior to the application of NCT to determine porosity density and distribution. Mass loss with time was measured daily (other than weekends) during the drying process. It has been reported [10] that drying to constant mass in an oven at 50 °C, whilst minimising microstructural changes, allows significant water transport in the capillary pore structure. It is also considered that such conditions, whilst unavoidable in expediting the drying process, could be experienced in an extreme, arid repository environment such as those that exist in countries such as Australia, South Africa and the USA.

### 2.2. Neutron radiography and tomography

The neutron imaging facility at the SAFARI-1 materials testing nuclear research reactor at Necsa, South Africa, was used to chart water transport through the wasteform.

Neutron radiography is a non-destructive examination (NDE) technique based on imaging using penetrating radiation to produce 2-D images, called radiographs, on samples under investigation. Being a non-destructive analytical tool, radiography enables the visualisation of interior features of objects without any physical modification of the object under investigation. The industrial system requires linear geometry setup of the radiation source, sample stage and detection system. When neutrons pass through an object they can be scattered, absorbed and transmitted. The transmitted component of the interaction is detected using radiography and provides information about materials that constitute the object under investigation according to the Beer–Lambert law:

$$I = I_0 e^{-\Sigma d}$$

where $I_0$ and $I$ are the intensities of the beam before and after interaction with the sample respectively, and $\Sigma$ and $d$ are the linear attenuation coefficient ($cm^{-1}$) and the thickness (cm) of the sample respectively. The linear attenuation coefficient is a function of the atomic number and energy (93% thermal neutrons at Necsa) which enables radiography to visualise material of different atomic numbers.

Neutron tomography is a 3-D non-destructive examination (NDE) technique based on reconstruction of a virtual 3-D image of the object under investigation using 2-D images obtained at different angles of rotation as the object under investigation is rotated through at least 180°.

The thermal neutron imaging facility at the SAFARI-1 reactor was used to map water transport through the cement applying radiography and tomography as analytical tools.

At 20 MW reactor power and using a 21 mm interior pinhole diameter neutron passage in the collimator, a 93% thermal neutron flux of $1.2 \times 10^7$ n $cm^{-2}$ $s^{-1}$ is delivered at the object position in the centre of the beam. Images are captured via a lithium-based zinc-sulphate scintillator screen using a Peltier-cooled Charged Coupled Device (CCD) camera with a $1024 \times 1024$ pixel array and 16-bit image output device. The system has a 2 μs/image readout capability. Using a 100 mm × 100 mm field of view (FOV), a resolution of 0.098 mm/pixel size is achieved [11]. This means that 2-D images (NR) have a 0.0096 $mm^2$, and 3-D images (NCT) a 0.0009 $mm^3$, spatial resolution limitation respectively at the 1 horizontal binning and 1 vertical binning of pixels. Binning of pixels horizontally and vertically on the CCD is the concept of grouping a number of pixels into one pixel, thereby affecting the intensity and the spatial resolution.

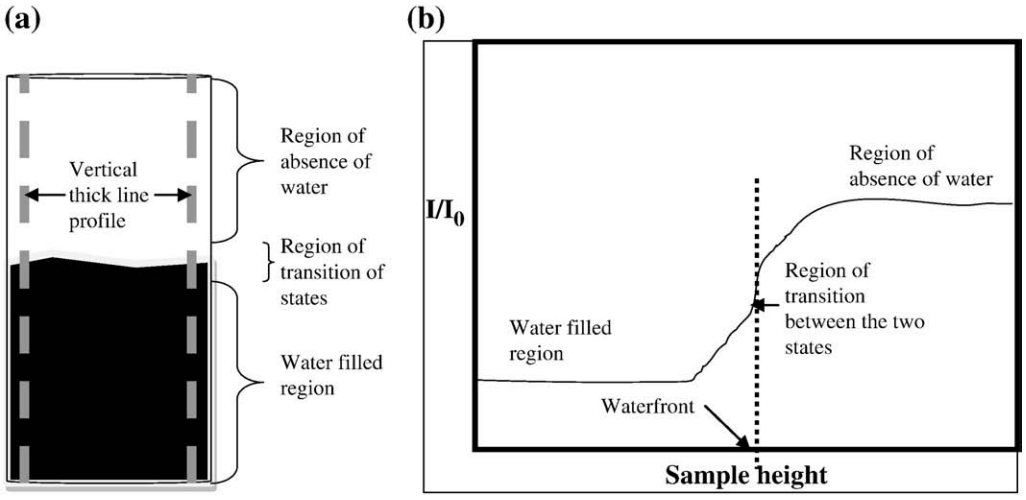


**Fig. 1.** (a) Schematic diagram of a radiograph showing a water front within a cylindrical mortar sample and (b) determination of the water front height from the resulting curve of intensity as a function of sample height.

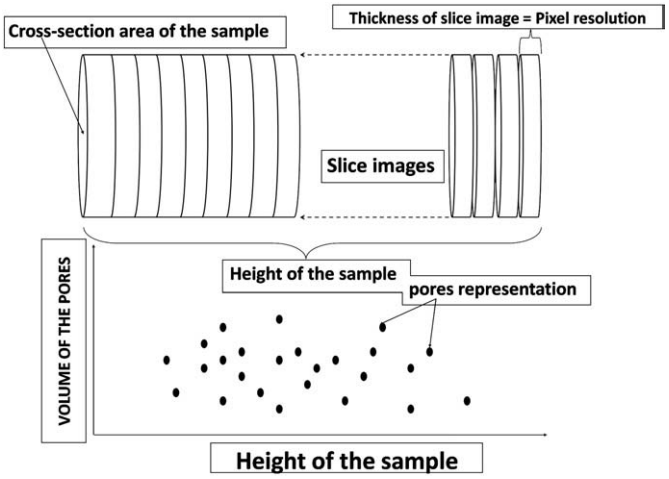


**Fig. 2.** (a) Schematic diagram showing the constitution of sample height from slice images and (b) presentation of pore size distribution as a function of sample height.

### 2.3. Sorptivity

Sorptivity measurements on the dried specimens, both un-leached and leached, were obtained from gravimetry according to the ASTM procedure [3], and from using 2-D neutron radiographs. In both methods, samples were tightly enclosed in aluminium tape with only the circular bottom faces of the samples exposed, facilitating water transport in one direction only (upwards). The exposed base of each sample was continuously immersed in water to a depth of approximately 2 mm and adsorption measured over periods of 1, 2, 4, 6, 9, 12, 16, 20 and 25 min, and for longer time periods (up to a month) where possible. The sorptivity, which is expressed as rate of water adsorption $I$ (mm), was computed from the linear mass gain as a function of the square root of time following the method outlined in reference [3]. In addition to the ASTM procedure detailed above sorptivity was also determined by neutron radiography. At the end of each time interval the samples were removed from the water, weighed and then transferred to the NR facility to collect 2-D radiographic data and chart water ingress. A rig was specially designed for the radiography facility so that the uncovered face of the samples remained immersed during data acquisition.

The 2-D images were obtained over a 3 second exposure time each with horizontal and vertical pixel binning settings of 4 and 1 respectively, resulting in spatial resolution limits of 0.391 mm/pixel and 0.098 mm/pixel respectively. The water could be visualised within each sample after each water absorption period, and a thick line profile was used to obtain intensity data from the sample image (Fig. 1a). From the curve of intensity as a function of the length of the sample, the water front could be determined as shown by dotted marker on Fig. 1b [12,13].

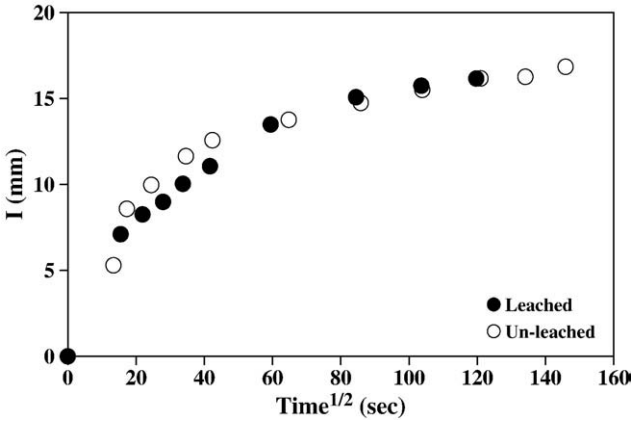


**Fig. 4.** Gravimetric sorptivity results of the un-leached and leached MTR wasteform.

### 2.4. Macro-pore distribution determination from NCT (3-D investigation)

The 3-D neutron tomography investigation was performed on completely dried specimens of the un-leached and leached MTR wasteform to determine macro-pore distributions. These 3-D images were obtained from the reconstruction of 360×2-D images acquired over a 20 second exposure period for each of the 2-D images.

A 3-D image (tomogram) is composed of slice images. The slice images are reconstructed from a series of radiographs (projections) taken at different angles of rotation of the sample. The reconstruction of slice images was performed using OCTOPUS software [14] and the analysis of 3-D image was carried out using VGStudio Max visualisation software [15].

OCTOPUS reconstructs cross-sectional images (slices) of the sample using a filter-back projection reconstruction algorithm. Image correction (background, electronic, beam hardening and beam fluctuation corrections) is carried out before the reconstruction. The result of reconstruction is a stack of slice images numbered according to their position on the sample from top to bottom, as depicted in Fig. 2a.

VGStudio Max visualisation software provides a 3-D visualisation and analysis of the stack of slice images. The stack is analysed as a 3-D image representation of the sample. Each region of the volume is represented by voxels (volume elements). The defect detection tool of VGStudio was used to detect pores and to provide their size and location inside the volume of the sample, as shown in Fig. 2b. The minimum pore

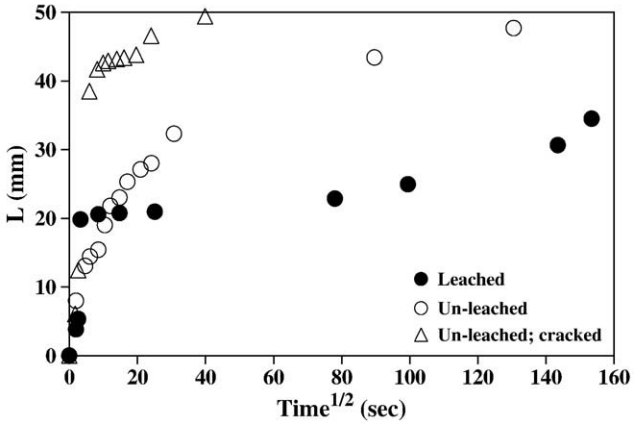


**Fig. 3.** Sorptivity results of the un-leached and leached MTR wasteforms based on NR analysis. A cracked sample with an extremely high water ingress rate is shown for comparative purposes.

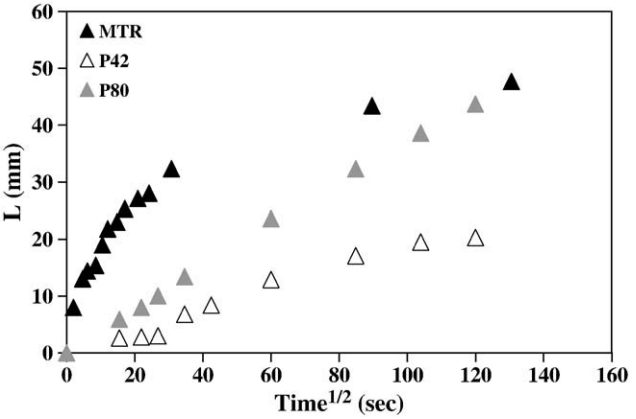


**Fig. 5.** Sorptivity determinations using NR of the MTR wasteform used in these studies with that of an OPC paste (P42 — water:cement of 0.42; P80 — water:cement of 0.80) used in previous studies [6].

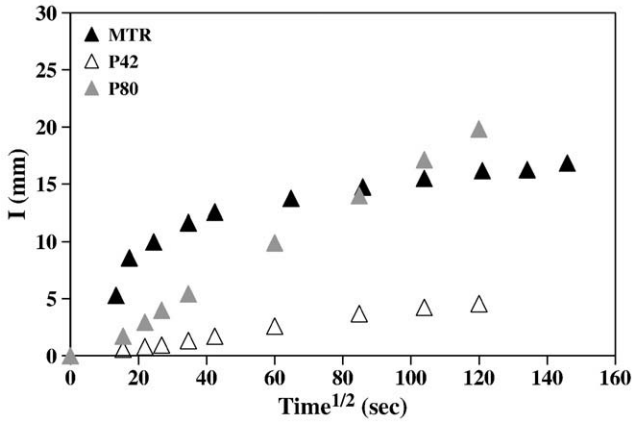


**Fig. 6.** Sorptivity by gravimetric measurements of the un-leached MTR wasteform used in these studies with that of an OPC paste (P42 — water:cement of 0.42; P80 — water: cement of 0.80) used in previous studies [6].

volume that can be detected is a voxel resolution and is equal to the product of $x$, $y$ and $z$ where $x$, $y$ and $z$ are the dimensional size of the voxel.

## 3. Observations and discussion

### 3.1. Sorptivity studies

Figs. 3 and 4 compare the sorptivity determined by NR and gravimetric methods respectively. The $y$-axes are labelled differently ($I$ and $L$ respectively) to distinguish between derived values obtained directly by the ASTM procedure and those calculated from a pixel intensity using NR.

The NR sorptivity experiments were generally carried out for about 8 h, although movement of water to fill the entire specimen was detected over a further 16 hour period. An experiment was also run on a severely cracked sample that was not originally intended for experimentation. The total time for the water to completely penetrate the severely cracked sample (signified as 'Un-leached; cracked' in Fig. 3) was just 10 min. It has been shown here to demonstrate the effect of extensive cracking on the rate of water movement through the wasteform. The NR results presented in Fig. 3 were obtained from the images shown later (2-D radiographs) using the procedures outlined in Section 2.3 [6,11].

The NR measurements show that for the initial sorption the sorptivity rate is greater for the leached wasteform than the un-leached. However after 2 min the un-leached sample continues to sorb whilst the leached wasteform sorption rate is much slower. After approximately 5 h water movement had reached 48 mm in the un-leached wasteform and 30 mm in the leached wasteform.

The difference between the water transport in the leached and un-leached wasteforms cannot be easily rationalised. It is suggested that perhaps water has solubilised and precipitated components during the 8 year leaching period altering the microstructure of the leached sample. What is evident is the ability of neutron radiography to so clearly distinguish between the water penetrations in such a definite way. We plan to further examine this difference in the future.

The sorptivity, as determined by gravimetry (see Fig. 4), is different to that determined using NR. Although gravimetry measurements were taken for much longer periods than those in the NR

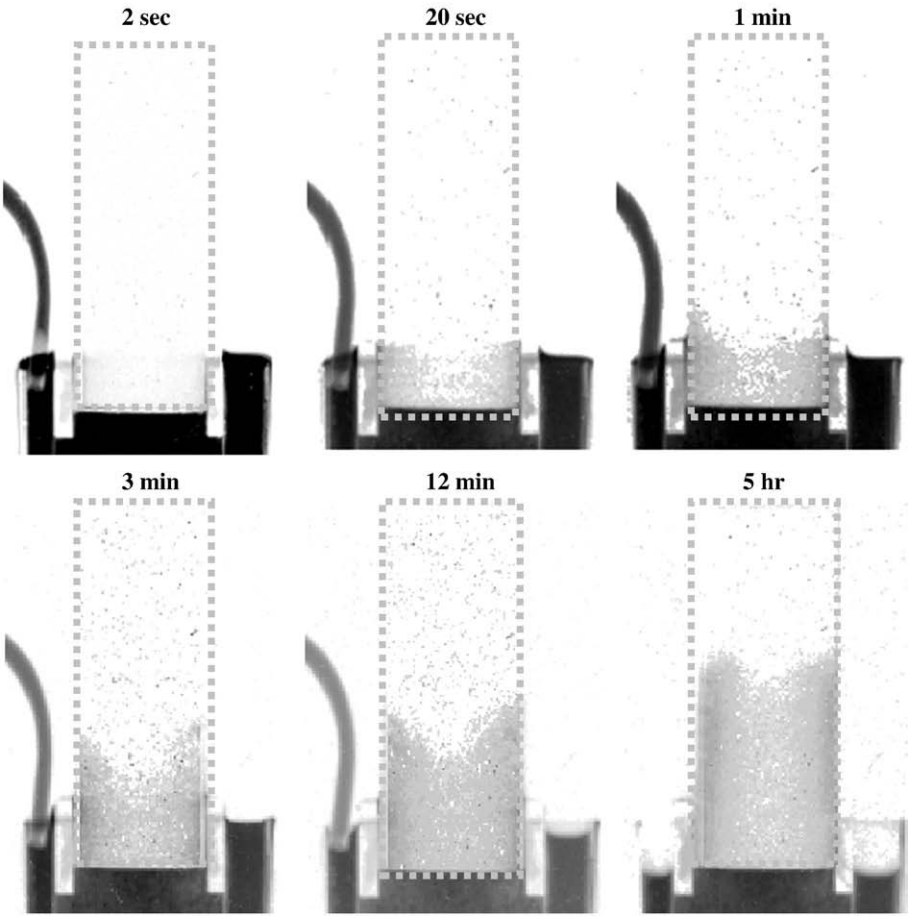


**Fig. 7.** Neutron radiographs depicting water front movement (darker tone) as a function of time in the un-leached MTR wasteform (outline of sample indicated by dotted line).

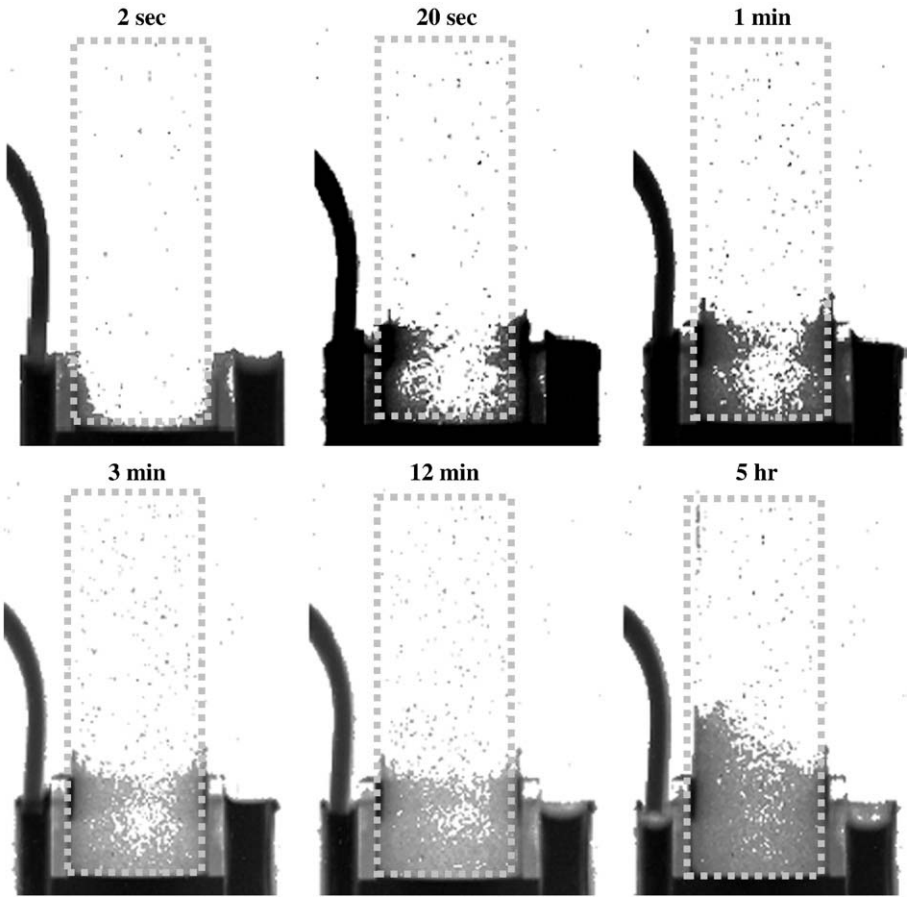


**Fig. 8.** Neutron radiographs depicting water front movement (darker tone) as a function of time in the leached MTR wasteform (outline of sample indicated by dotted line).

experiments, for comparison purposes we have only plotted data to about 6 h. The gravimetric determinations are similar for the un-leached and leached samples, and after 5 h the calculated water movement is about 16 mm for both the leached and un-leached specimens. They are a factor of three lower for the un-leached wasteform when compared to the NR calculated value, and a factor of two lower for the leached wasteform when compared to the NR measurement.

The sorptivity results of the un-leached MTR wasteforms used in these studies were compared to results obtained in another study [6] on cylinders of paste (about 25 mm diameter and 50 mm high) made of OPC and water, one with a water to cement (w/c) ratio of 0.42 and another with a ratio of 0.80. Fig. 5 compares the sorptivity of the MTR wasteform, as determined by NR analysis, with those of the OPC pastes. The MTR wasteform has a higher rate of sorptivity than both the OPC samples, although is similar to the OPC with a w/c of 0.8 after about 4 h.

Fig. 6 makes the same comparison using gravimetric sorption. In this instance the MTR wasteform has a higher sorptivity than the OPC paste with a w/c of 0.42, but after two hours the sorptivity of the OPC paste with a w/c of 0.80 has a higher sorptivity than the MTR wasteform.

The gravimetric values for both sets of sorptivity experiments are typically lower than those determined using NR, as shown in Figs. 3 to 6. This difference is not surprising as NR visualises the actual position and the ASTM method calculates the value of water movement.

### 3.2. 2-D neutron imaging

Figs. 7 and 8 display NR images visualising the water front progress as it moves through the sample microstructure, after specific time periods, of the un-leached wasteform and a wasteform originally leached for 8 years.

The images in the figures show the cylindrical wasteform cylinder in the centre (outline indicated by dotted line), and the base of the water reservoir (shown in dark contrast) in which the samples stand and, in some cases, the tubing (on the left) which carried the water to the reservoir during the experiments. The darker contrast in the images is due to the greater neutron attenuation capacity of the water.

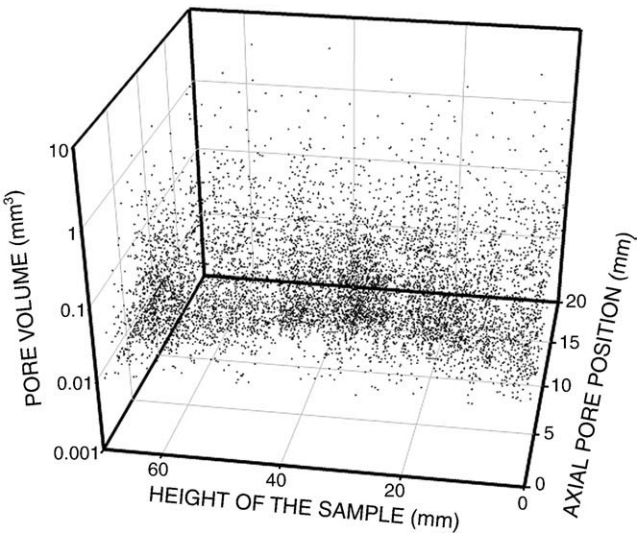


**Fig. 9.** Macro-pore volume distribution as a function of depth and axial position within the un-leached MTR wasteform.

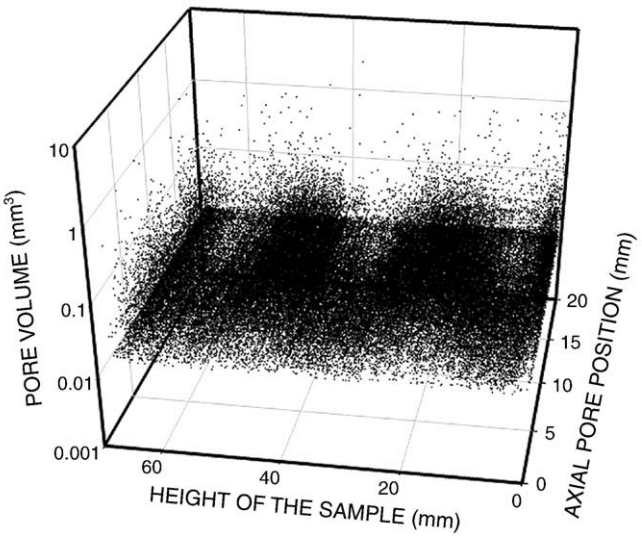


**Fig. 10.** Macro-pore volume distribution as a function of depth and axial position within the leached MTR wasteform.

As only one experimental rig was available for carrying out the sorptivity testing, the samples could not be analysed simultaneously.

For the analyses of the un-leached wasteform (Fig. 7) and the leached wasteform (Fig. 8), the results verify the sorptivity calculations above, in that the un-leached wasteform visually has a greater sorptivity rate than that for the leached sample.

The NR results could not highlight any significant differences in water movement between the 800 μm surface layer and the interior of the two samples, at least not at the spatial resolution in the images above. Resolving any differential in sorptivity between the thin surface layer and the underlying matrix was difficult due to the relatively rapid water movement through the wasteform.

### 3.3. Macro-pore size and pore distribution by NCT

Figs. 9 and 10 present the macro-pore size distribution plots as a function of depth and axial position within the dried un-leached and leached wasteform samples respectively obtained from the neutron tomograms through OCTOPUS Reconstruction Software and VGStudio visualisation software [14,15]. In the figures, each data point indicates a detected pore with the given volume. Thus the number of points reflects the number of pores; the *y*-axis indicates the pore size; the *x*-axis the pore size distribution along the length/height of the sample; and the *z*-axis the spread of pores axially. Although overall pore volume can be calculated from analysis of the data, it cannot be considered as the true total pore volume as the resolution of the technique can only effectively measure pores with a diameter greater than about 0.098 mm.

The macro-pore size distribution in both the un-leached and leached wasteform samples mostly lies between 0.01 and 1 $mm^3$. For the un-leached sample, 88% of the pores have a volume less than 0.1 $mm^3$, whilst for the leached sample 95% of the pores have a volume less than 0.1 $mm^3$. The leached wasteform has a higher density of smaller pores throughout its entire length. The relatively dense lines of pores at about 0.01 $mm^3$ in both samples probably represent sub-vertical cracks passing through almost the entire specimen.

There are several outlying higher results for both samples that are more likely cracks than pores. These values do not appear on Figs. 9 and 10 in order to keep the pore volume range to four orders of magnitude (to aid visualisation of the data). In the un-leached MTR wasteform, for example, a total volume equating to approximately 6 $cm^3$ has been calculated near the top of the specimen. This highlights the capability of neutron tomography in identifying such cracks, and their position, since a crack of this magnitude will likely dominate sorptivity until filled, especially if it is located near the water–solid interface.

The ability to define the macro-pore distribution is one of the major advantages of NCT. It is of considerable interest that the macro-pore distribution is reasonably even in both samples showing that matrix segregation has not occurred. In addition, the technique can give useful information on the position and density of the macro pores showing how they may contribute to water transmission.

### 3.4. Neutron tomography (3-D imaging)

Complementary to the macro-pore size distribution plots, NCT can give a detailed reconstruction and 3-D visualisation of the pore and crack microstructure in the sample. Images of this are shown in Figs. 11 and 12 for the un-leached and the leached wasteforms respectively. They depict portions of a continuous crack and

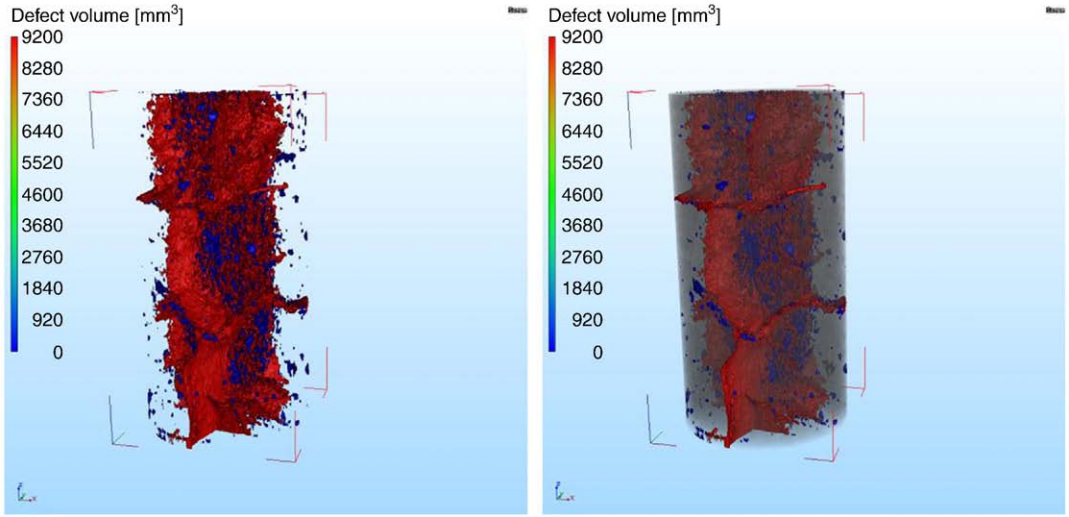


**Fig. 11.** Neutron tomographic image of the un-leached MTR wasteform which was tested for sorptivity with water using NR. The image on the left represents the total void visualisation with the red colouration corresponding to cracks, grading to blue for fine cracks and unconnected pores. The image on the right has the outline of the wasteform cylinder superimposed for context.

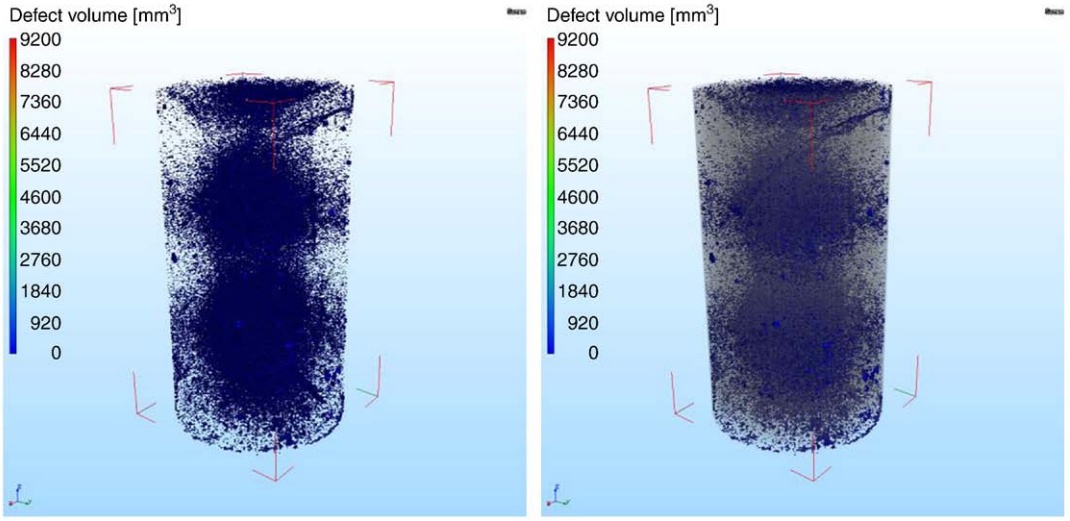


**Fig. 12.** Neutron tomographic image of the leached MTR wasteform which was tested for sorptivity with water using NR. The image on the left represents the total void visualisation with the blue colouration corresponding to pores. The image on the right has the outline of the wasteform cylinder superimposed for context. Note the lower pore connectivity/cracks compared to the un-leached sample.

indications of the void volumes within the sample. In order to understand the complete void structure, a computer generated 'avi' files (Supplementary materials) have to be viewed to give the three dimensional representation and the pictures here give an incomplete albeit striking portrayal of the structure.

The visualisations correlate well with the respective sorptivity rates for the un-leached and leached wasteforms, the apparent greater void volume and connectivity of the pores and cracks in the un-leached sample reflected in its higher sorptivity rate.

## 4. Conclusions

The diffusion of radioactive ions from cementitious wasteforms is generally measured by leaching which is related to that rate which water can penetrate into that wasteform. The utility of neutron radiography and tomography to measure the rate of water penetration was demonstrated here. Neutron tomography showed both the porosity and the extent of the cracking that had occurred in an 8 cm high cylinder of 4 cm diameter. The rate of the measured water penetration, as measured both by sorptivity and neutron imaging, was generally greater than that found on pastes made of Ordinary Portland Cement with water to cement ratios of 0.42 and 0.80.

The potential for the cracks in a mechanically damaged specimen to distribute the water through the sample in a very short time was also demonstrated. The extent of water penetration calculated by gravimetry (as per the ASTM Sorptivity procedure) was underestimated in comparison to that determined by neutron radiography.

The structural variations in an MTR wasteform, one un-leached and one leached for about 8 years, have been differentiated by both NR and NCT. The lower sorptivity rate exhibited by the leached wasteform shown by NR correlates with the hypothesis that leaching in water had modified the structure of the wasteform. Although there are more individual pores within the leached sample compared to the un-leached sample, there is seemingly a lower pore connectivity and lower crack density in the leached sample, leading to lower water transmissivity properties compared to the un-leached sample. The mechanism for the alteration of the wasteform is unclear, but neutron imaging has clearly defined an issue that requires further investigation.

The studies presented here highlight the significant potential of neutron imaging, particularly 3-D neutron tomography, in the investigation of cementitious materials used for many purposes, not just wasteforms. The technique has the advantage of visualising and measuring, non-destructively, the water distribution within macroscopic samples and to describe their inherent processes.

## Appendix A. Supplementary data

Supplementary data associated with this article can be found, in the online version, at doi:10.1016/j.cemconres.2010.03.011.

## References

[1] P.J. McGlinn, D.R.M. Brew, Laurence P. Aldridge, T.E. Payne, K.P. Olufson, K.E. Prince, I.J. Kelly, Durability of a cementitious wasteform for intermediate level waste, Materials Research Society (MRS) Symposium on the Scientific Basis for Radioactive Management XXXI, Mater. Res. Soc. Symp. Proc., vol. 1107, 2007, pp. 101–108.
[2] S.J. Desouza, R.D. Hooton, J.A. Bickley, Evaluation of laboratory drying procedures relevant to field conditions for concrete sorptivity measurements, Cement, Concrete and Aggregates 19 (2) (1997) 59–63.
[3] ASTM, C1585-04, Standard Test Method for Measurement of Rate of Adsorption of Water by Hydraulic-Cement Concretes, American Society for Testing and Materials (2004).
[4] F.C. De Beer, M.F. Middleton, J. Hilson, Neutron radiography of porous rocks and iron ore, Applied Radiation and Isotopes 61 (2004) 487–495.
[5] F.C. De Beer, J.J.L. Roux, E.P. Kearsley, Testing the durability of concrete with neutron radiography, Nuclear Instruments and Methods in Physics Research A 542 (2005) 226–231.
[6] D. R. M. Brew, F. C. De Beer, M. J. Radebe, R.Nshimirimana, P. J. McGlinn, L. P. Aldridge, T.E.Payne, Water transport through cement-based barriers — preliminary studies using neutron radiography and tomography, Nuclear Instruments and Methods A — submitted October 2008.
[7] P.B. Carter, UKAEA (Dounreay), Manual for process qualification of cemented MTR raffinate at the Dounreay cementation plant, Report No. WSSD(99)P24, unpublished technical note (2000).
[8] C.G. Howard, D.J. Lee, UKAEA (Winfrith), Immobilisation of MTR waste in cement (product evaluation), Final Report No. AEEW-R 2312, 1987.
[9] E. Revertegat, C. Richet, P. Gégout, Effect of pH on the durability of cement pastes, Cement and Concrete Research 22 (1992) 259–272.
[10] L.J. Parrott, Moisture conditioning and transport-properties of concrete test specimens, Materials and Structures 27 (172) (1994) 460–468.
[11] F.C. De Beer, Characteristics of the neutron/X-ray tomography system at the SANRAD facility in South Africa, Nuclear Inst. Methods Phys. Res. A 542 (1–3) (2005) 1–8.
[12] F.C. De Beer, W.J. Strydom, E.J. Griesel, The drying process of concrete: a neutron radiography study, Applied Radiation and Isotopes 61 (2004) 617.
[13] P. Zhang, F.H. Wittmann, T.J. Zhao, E. Lehmann, P. Vontobel, S. Hartmann, Restoration of Buildings and Monuments, vol. 15, 2009, pp. 91–100.
[14] B. Masschaele, M. Dierick, J. Vlassenbroeck and Y De Witte, *Octopus V8*. Ghent: Institute for Nuclear Science (INW), XRayLab (2007). Available on-line http://www.xraylab.com.
[15] Volume Graphics GmbH *VGStudioMax 1.2.1*. Germany (2006) Available on-line http://www.volumegraphics .com/products/vgstudio/index.html